NASA TECHNICAL NOTE

NASA TN D-7657

NASA TN D-7657

WICKING OF LIQUIDS IN SCREENS

by Eugene P. Symons

Lewis Research Center

Cleveland, Ohio 44135

NATIONAL AERONAUTICS AND SPACE ADMINISTRATION • WASHINGTON, D. C. • MAY 1974

1. Report No.	2. Government Accession No.	3. Recipient's Catalog No.
NASA TN D-7657		

4. Title and Subtitle	5. Report Date
WICKING OF LIQUIDS IN SCREENS	MAY 1974
	6. Performing Organization Code

7. Author(s)	8. Performing Organization Report No.
Eugene P. Symons	E-7781
	10. Work Unit No.
9. Performing Organization Name and Address	502-24
Lewis Research Center National Aeronautics and Space Administration Cleveland, Ohio 44135	11. Contract or Grant No.
	13. Type of Report and Period Covered
12. Sponsoring Agency Name and Address	Technical Note
National Aeronautics and Space Administration Washington, D.C. 20546	14. Sponsoring Agency Code

15. Supplementary Notes

16. Abstract

This report presents the results of an investigation conducted to determine the magnitude of the wicking rates of liquids in various screens. Evaluation of the parameters characterizing the wicking process resulted in the development of an expression which defined the wicking velocity in terms of screen and system geometry, liquid properties, and gravitational effects. Experiment data obtained both in normal gravity and in weightlessness demonstrated that the model successfully predicted the functional relation of the liquid properties and the distance from the liquid source to the wicking velocity. Because the pore geometry in the screens was complex, several screen geometric parameters were lumped into a single constant which was determined experimentally for each screen.

17. Key Words (Suggested by Author(s))	18. Distribution Statement
Fluid flow Wicking Weightlessness Capillarity	Unclassified - unlimited Category 12

19. Security Classif. (of this report)	20. Security Classif. (of this page)	21. No. of Pages	22. Price*
Unclassified	Unclassified	31	$3.25

* For sale by the National Technical Information Service, Springfield, Virginia 22151

WICKING OF LIQUIDS IN SCREENS

by Eugene P. Symons

Lewis Research Center

SUMMARY

A study was conducted to determine the magnitude of the wicking rates of liquids in various screens. An analytical model of the wicking process was developed which expressed the wicking velocity as a function of such system parameters as liquid properties, gravitational effects, and geometric effects. Experiment data acquired both in normal gravity and in weightlessness demonstrated that the model developed predicted the correct functional dependence of several parameters important in the wicking process. In particular, the functional relation to the wicking velocity of the liquid properties and the distance along the screen from the liquid source was verified experimentally. However, because the geometry of the pores within the screen was complex, it was necessary to lump several screen geometric parameters into a single geometric constant. This constant was determined experimentally for each screen mesh evaluated in this study.

INTRODUCTION

The use of capillary containment devices (i.e., screens or wire cloth) for the efficient control and transfer of liquids, both cryogenic and noncryogenic, in reduced- and zero-gravity environments has received considerable mention in the literature. The effective operation of these devices depends on the containment device being maintained in a filled condition.

The phenomenon of capillary wicking in screens is important both in obtaining and maintaining a filled containment device. High wicking rates are undesirable for a refilling or filling application since the wicking fluid may seal the screen before complete filling is obtained and, thus, compromise the effectiveness of the device. If warm gas is used for the pressurization of cryogenic propellant tanks, it is probable that some portion of a filled containment device may dry out because of liquid evaporation at the screen surface. It is conceivable that such a situation could be prevented by wicking rates which

are of sufficient magnitude to replace any liquid evaporated at the screen. Thus, the determination of wicking rates is of considerable importance in the effective design of any capillary containment device.

To date, the extent of information available concerning the wicking of liquids in screens is somewhat limited. Reference 1 examines wicking as a solution to the problem of evaporation from a screen device. A mathematical model was postulated and data were obtained for four dutch twill screens using pentane as the test liquid. The data were obtained in a horizontal wicking chamber and examined wicking flow parallel to the warp wires. The equations presented in the model were generally unsuccessful in predicting the magnitudes of the observed wicking rates. Reference 2 also presents an analysis for wicking and data for a single test conducted with 375×2300 mesh dutch twill screen. Both references conclude that the wicking rates observed were small.

This report presents the results of a study to determine the wicking rates of liquids in screens. As a part of the study, an analytical model was developed which expresses the wicking velocity as a function of various system parameters. Because of the complex geometry of the pores in all the screen materials that exhibited wicking, it was necessary to lump the screen parameters into a single geometric constant in the analytical model. The experiment data are compared with the model, and the geometric constants were determined experimentally for eight twilled-weave and two plain-weave dutch screens. These constants are compared, where possible, with those obtained in reference 1. This report provides the user with appropriate wicking rates for a wide range of screen meshes.

Experiment data were taken in both normal gravity and zero gravity. All zero-gravity data were obtained in the Lewis Research Center's 2.2-Second Drop Tower Facility, which is described in the appendix.

SYMBOLS

A_F cross-sectional area for wicking flow, cm^2

A_S area of screen surface, cm^2

A_T total cross-sectional area of screen, cm^2

a acceleration, cm/sec^2

c correlation constant, μm

D tube diameter, cm

D_s manufacturer's rated pore size, μm

$\dot{G}$ evaporation rate, g/sec/cm

h	height of capillary rise, cm
K_1	permeability of screen, cm^2
L	distance from wicking front to liquid source, cm
$\dot{m}$	mass rate, g/sec
ΔP_c	capillary driving pressure, N/cm^2
ΔP_f	frictional pressure drop, N/cm^2
ΔP_g	gravitational pressure head, N/cm^2
p	porosity of screen
$\dot{Q}$	applied heat rate, J/sec
q	volumetric flow rate, cm^3/sec
R, R_1, R_2	radii of curvature, cm
t	time, sec
V_w	wicking velocity, cm/sec
V_x	local wicking velocity, cm/sec
W	screen width, cm
x	intermediate location
α	angle of screen inclination with respect to horizontal, deg
δ	screen thickness, μm
θ	contact angle of liquid on screen material, deg
λ	latent heat of vaporization, J/g
μ	liquid viscosity, g/cm/sec
ρ	density of liquid, g/cm^3
σ	surface tension, N/cm
φ	constant

ANALYSIS OF WICKING FLOW

As was done in reference 3, it shall be assumed that wicking is occurring in the absence of evaporation and that wicking flow in a screen is governed by the same equations used to predict capillary rise in tubes.

At any liquid-vapor interface, the surface behaves as if it were a contractable membrane existing in tensile stress. The force per unit length tending to contract the surface is defined as the surface tension σ. The pressure difference which exists across the liquid-vapor interface can be described as a function of the surface tension and the curvature of the surface by the Young and Laplace equation:

$$\Delta P_c = \sigma \left(\frac{1}{R_1} + \frac{1}{R_2} \right)$$

where R_1 and R_2 are the principal radii of curvature of the liquid-vapor interface.

If the tube is circular in cross section, R_1 and R_2 are equal and the previous equation becomes

$$\Delta P_c = \frac{2\sigma}{R}$$

The radius of curvature in a tube of circular cross section may be expressed as a function of the tube diameter D and the contact angle θ (sketch (a)):

$$R = \frac{D}{2 \cos \theta}$$

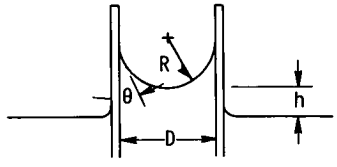

(a)

After substituting, the capillary pressure difference across the liquid-vapor interface for a tube of circular cross section may be expressed as

$$\Delta P_c = \frac{4\sigma \cos \theta}{D}$$

Because the pattern formed in the weaving of typical wicking screens (i.e., dutch weaves) is complex, the actual pores in the screen through which the liquid rises are not circular in cross section. In fact, the pores in such a screen are of a very complex shape, which does not lend itself to any rigorous calculation of the actual radii of cur-

vature which might exist at the wetted pore. Thus, it becomes necessary to determine an equivalent circular pore size experimentally. This is generally done by determining the screen bubble point, which is defined as the liquid head which can be supported at the liquid-vapor interface in the screen pores before vapor bubbles break through the interface.

The previous equation may then be expressed as

$$\Delta P_c = \frac{\varphi\sigma \cos\theta}{D_s} \tag{1}$$

($\varphi = 4$ for circular pores.) If the screen wick is acting in the presence of a gravitational field, the pressure differential caused by this field may be expressed (see sketch (b)) as

$$\Delta P_g = \rho a L \sin\alpha \tag{2}$$

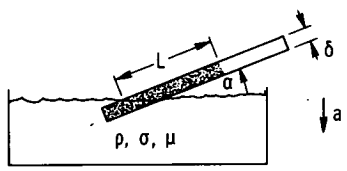

(b)

In the case of the rise of liquid in a capillary tube, the frictional pressure differential associated with the viscous losses over a length L has generally been expressed by the Poiseuille formulation for frictional pressure loss $32\mu LV/D^2$. This is not rigorously correct since the phenomenon of capillary rise is, in fact, an example of unsteady flow (the velocity of the fluid in the tube at any given position decreases with time as the liquid rises in the tube) and the Poiseuille formula assumes steady laminar flow. However, it does include those terms which should affect the actual losses which occur. However, this formulation, when applied to wicking in screens, would make no provision for the fact that liquid flows around the cylindrical wires within the screen and thereby creates differing flow areas depending upon whether the wicking occurs perpendicular or parallel to the warp wires. As a result, a better approximation might be made by using Darcy's law for steady laminar flow in a porous media:

$$\Delta P_f = \frac{q\mu L}{K_1 A_T} = \frac{V_w A_F \mu L}{K_1 A_T} \tag{3}$$

Unsteady terms, such as the pressure drop associated with the rate of change of momentum are neglected in the model. Equations (1) to (3) are then the basic equations that should characterize wicking flow in a screen. The capillary pressure tends to impart motion, while the other terms tend to retard it:

$$\Delta P_c = \Delta P_g + \Delta P_f$$

or

$$\frac{\varphi\sigma \cos\theta}{D_s} = \rho a L \sin\alpha + \frac{V_w A_F \mu L}{K_1 A_T} \tag{4}$$

Equation (4) may then be solved (with $\theta = 0^o$) for the wicking velocity:

$$V_w = \frac{\varphi K_1}{D_s}\left(\frac{A_T}{A_F}\right)\left(\frac{\sigma}{\mu}\right)\frac{1}{L} - \frac{K_1 \rho a \sin\alpha}{\mu}\left(\frac{A_T}{A_F}\right) \tag{5}$$

And the time as a function of interface position is obtained by integrating equation (5) with $L = 0$ at $t = 0$

$$t = \frac{\varphi\mu\sigma}{D_s K_1 \rho^2 a^2 \sin^2\alpha}\left(\frac{A_F}{A_T}\right) - \frac{\mu L}{K_1 \rho a \sin\alpha}\left(\frac{A_F}{A_T}\right) - \frac{\varphi\mu\sigma}{K_1 D_s \rho^2 a^2 \sin^2\alpha}\left(\frac{A_F}{A_T}\right)$$

$$\times \log\left[\frac{\varphi K_1}{D_s}\left(\frac{\sigma}{\mu}\right)\frac{A_T}{A_F} - \frac{K_1 \rho a \sin\alpha}{\mu}\frac{A_T}{A_F} L\right] \tag{6}$$

For zero-gravity wicking, or for wicking in a horizontally oriented screen in a gravitational field, equation (5) becomes

$$V_w = \frac{\varphi K_1}{D_s}\left(\frac{A_T}{A_F}\right)\left(\frac{\sigma}{\mu}\right)\frac{1}{L} \tag{7}$$

and the time as a function of interface position is

$$t = \frac{D_s}{\varphi K_1}\left(\frac{A_F}{A_T}\right)\left(\frac{\mu}{\sigma}\right)\frac{L^2}{2} \tag{8}$$

EXPERIMENT APPARATUS

In order to support the equations presented herein, an experimental investigation was conducted in which several screens and liquids were evaluated to determine their wicking characteristics.

Test Liquids and Screen Samples

The two liquids employed in the experimental investigation were methanol and ethanol. Their properties pertinent to this study are presented in table I. Both liquids exhibited a near zero-degree static contact angle on the stainless-steel screen material, thus simulating the contact angle of typical propellants on the screen material.

A series of 13 different screen meshes were evaluated in the experimental study. These consisted of eight twilled-weave dutch meshes (20×250, 30×500, 165×800, 200×600, 80×700, 165×1400, 200×1400, and 325×2300), two plain-weave dutch meshes (24×110 and 50×250), and three square meshes (150×150, 200×200, and 400×400). Samples of each screen to be tested were cut in strips approximately 2.54 centimeters (1 in.) wide by 30.48 centimeters (12 in.) long. For each of the dutch-weave screens, two samples were cut, one with the warp wires running parallel to the screen width and one with the warp wires running perpendicular to the screen width. Microphotographs showing the difference between the plain-weave and twilled-weave dutch screens are presented in figure 1.

Horizontal Wicking Chamber

The chamber used to obtain liquid wicking velocities in horizontally oriented screen samples is shown in figure 2. The chamber consisted of a liquid reservoir mounted to a base plate which was equipped with four leveling bolts positioned at each corner. The upper edge of the liquid reservoir was machined so as to be parallel to the base plate to within 0.008 centimeter per meter (0.001 in./ft). The screen sample to be evaluated was attached at one end to a mounting block located within the reservoir by two small screws and clamped between two aluminum blocks at the opposite end. The blocks were positioned on two threaded rods so that the screen sample could be oriented in a horizontal position. Each sample was so positioned and checked with a precision level accurate to within 0.008 centimeter per meter (0.001 in./ft). A small scale having divisions of 0.1 centimeter was located in the same plane as the screen sample and was used to measure the displacement of the wicking liquid as a function of time. Liquids could be

added to the reservoir through a burette which extended through a Plexiglas cover. The cover was positioned over the base plate and the screen sample in an attempt to minimize evaporation from the screen surface during the wicking tests. Elapsed time was measured with a precision timer accurate to ±0.01 second.

Experiment Drop Package

The experiment drop package used to obtain wicking rates in zero gravity is shown in figure 3. The package is a self-contained unit consisting of the liquid reservoir and screen sample, a photographic system, a timing light generator, and an electrical system to operate the various components. A backlighting system provided indirect illumination of the screen sample with a focused light source to permit photographic recording of the leading edge of the wicking liquid on 16-millimeter motion-picture film. A timing light generator placed a timing mark on the film every 0.01 second to provide an indication of elapsed time. The liquid reservoir was fabricated so that liquid would contact the screen only after the system entered zero gravity. This condition was achieved by using capillary pumping (fig. 3). The bulk liquid was contained in a cylindrical reservoir with an inside diameter of 7.95 centimeters ($3\frac{1}{8}$ in.) and a length of 11.40 centimeters ($4\frac{1}{2}$ in.). A smaller cylinder 3.81 centimeters ($1\frac{1}{2}$ in.) in diameter and 8.9 centimeters ($3\frac{1}{2}$ in.) in length was positioned within and concentric to the larger container. This smaller cylinder was fabricated in two sections along a plane parallel to the longitudinal axis. A slot 0.254 centimeter by 2.54 centimeters (0.1 in. by 1 in.) was machined at the joint of the two sections. The sections were held in place by four screws. The screen sample was positioned within the slot and held in position by two of the screws. Both absorbent tissue and rubber were used to space the screen approximately equidistant from the sidewalls of the slot. They also provided a means of damping out any initial transients imparted to the wicking liquid by the capillary rise of the liquid within the slot in zero gravity. No differences were observed in the data obtained. Liquid displacements were obtained from the data film by using a Vanguard motion analyzer.

The timing-light generator, the camera, the lights, and all other electrical components were operated through a control box and received their power from rechargeable nickel-cadmium cells.

Cleaning Procedure

Prior to each wicking test, the screen strip to be tested was cleaned in a class 10 000 clean-room environment. Each strip was immersed in a filtered nitric acid solution at room temperature for 10 minutes. It was then thoroughly flushed with filtered de-

ionized water and dried in a warm-air dryer. In the following step, each strip was flushed with filtered methanol, rinsed with filtered de-ionized water, and dried. As a final step, each screen sample was individually sealed in a clear plastic wrapper and microscopically examined for particulate content.

EXPERIMENT RESULTS AND DISCUSSION

Wicking in Weightlessness and Horizontally Oriented Screens

According to the equations put forth in the analysis section of this report, the wicking velocity of a liquid in a screen in a weightless environment or in a horizontal orientation can be expressed as (eq. (7))

$$V_w = \frac{\varphi K_1}{D_s}\left(\frac{A_T}{A_F}\right)\left(\frac{\sigma}{\mu}\right)\frac{1}{L}$$

Two parameters in the preceding expression (K_1 and A_F) cannot be measured and, thus, all the screen geometric parameters are lumped into a single correlation constant c.

$$V_w = \frac{c}{L}\left(\frac{\sigma}{\mu}\right)$$

In order to validate this expression, all the screen samples were tested in the experiment drop package in zero gravity as well as in the wicking chamber in which the screens were oriented horizontally. Unfortunately, except for those screens which exhibited good wicking characteristics, the total distance that the liquid wicked in the screen during the available zero-gravity time of 2.2 seconds was not sufficient to determine accurately the magnitude of the wicking rate.

Several photographs showing screen samples in which sufficient wicking occurred are presented in figure 4. Figure 4(a) shows a 50×250 plain-weave dutch screen in which a total wicked distance of 0.87 centimeter was obtained in 1.16 seconds. Figure 4(b) shows a 200×600 twilled-weave dutch screen in which the total wicked distance was 0.79 centimeter in 1.20 seconds. These distances are typical of those obtained with the better wicking screens. It was expected that square-mesh screen would not wick since the nature of the weave provided no wicking path for the liquid. Several tests were conducted in zero gravity which confirmed this contention.

If the preceding equation expresses the correct functional relation of the parameters, the wicking velocity should be inversely proportional to the distance from the liquid

source. Hence, a plot of wicking velocity against distance from the liquid source should be linear on log-log paper and have a negative unit slope. Such a plot is presented in figure 5 for an 80×700 twilled-weave dutch screen in which the wicking liquid was methanol and the wicking was parallel to the warp wires. This plot is typical of the data obtained in weightlessness for both the twilled-weave and plain-weave dutch screens.

In order to demonstrate that wicking rates obtained in zero gravity and those obtained in horizontally oriented screens in a normal-gravity environment were identical, all screens which exhibited good wicking characteristics in the zero-gravity tests were tested in the horizontal position in normal gravity. The results are compared in figure 6 for an 80×700 twilled-weave dutch screen in which the wicking liquid was methanol and the direction of wicking was parallel to the warp wires. This plot is typical of the data taken and shows excellent agreement between the zero-gravity and horizontal data.

Since the data taken in normal gravity with the screen oriented horizontally were not time limited as were the zero-gravity data, it was possible to obtain wicking rates for all the dutch weave samples. Data plots similar to those shown in figures 5 and 6 were prepared by dividing the distance from the liquid source by the ratio of surface tension to viscosity. The results are shown in figure 7 for wicking flow parallel to the warp wires and in figure 8 for wicking flow perpendicular to the warp wires. In most cases, the wicking velocities are greater for a given screen when wicking is parallel to the warp wires. This result is to be expected since the nature of the weave is such that this path would normally create less restriction for flow. Of the eight twilled-weave dutch screens tested, six behaved in this manner. The two exceptions were 200×600 mesh and 165×800 mesh (not shown in either figure). No explanation can be given for the observed behavior. However, it may be significant that these screens were the only screens tested in which the ratio of the number of shute wires to the number of warp wires per inch was less than 5.

Three of the screens evaluated in this study were also examined in reference 1. The observed results are compared in figure 9. The observed wicking velocities in this study were about 180 percent greater, 20 percent greater, and 33 percent less than those of reference 1 for 80×700, 165×400, and 200×600 mesh screens, respectively. Observed differences could be caused in part by the difference in experimental technique. In reference 1, data were taken with pentane by equating evaporation rate to wicking rate. The experimental method was dependent on a thermal analysis of the wicking apparatus to determine what percentage of the applied heat was employed in the evaporation of the test liquid. In this investigation, the wicking rates were determined by visually observing the position of the advancing liquid front as a function of time.

Correlation constants obtained for all the screens tested which exhibited wicking characteristics are presented in table II, along with some geometric data. No data are shown for the square-mesh screens since these screens did not wick.

Gravitational Effects on Wicking

Although the main emphasis of this study was the determination of wicking rates in weightlessness, several tests were conducted in which an attempt was made to investigate the effect of gravity on the wicking rate of the liquid in the screen. According to equation (5) of the analysis section, the wicking velocity in any gravitational environment may be expressed as

$$V_w = \frac{\varphi K_1}{D_s}\left(\frac{A_T}{A_F}\right)\left(\frac{\sigma}{\mu}\right)\frac{1}{L} - K_1 \sin\alpha\left(\frac{A_T}{A_F}\right)\left(\frac{\rho a}{\mu}\right)$$

or in terms of the correlation constant c as

$$V_w = \frac{c}{L}\left(\frac{\sigma}{\mu}\right) - c\left(\frac{\rho a}{\mu}\right)\frac{D_s}{\varphi}\sin\alpha$$

If this equation is valid, a plot of the wicking velocity against $1/L$ should be a straight line on rectangular grid with a slope of $c(\sigma/\mu)$ and should intercept the $V_w = 0$ axis at $1/L$ equal to $(\rho a D_s/\varphi\sigma)\sin\alpha$.

Data obtained for a vertically oriented 80×700 twilled-weave dutch screen in which the wicking liquid was ethanol and the wicking was perpendicular to the warp wires are shown in figure 10. The line drawn through the data has a slope of $c(\sigma/\mu)$ and intercepts the abscissa at $1/L = \rho a D_s/\varphi\sigma$. As shown, the line represents the data quite well except at small values of $1/L$ (large values of L). This may be caused in part by the fact that evaporation would be more significant as the distance from the source increases. Tests were also run 165×1400 and 200×600 twilled-weave dutch with both screens vertically oriented and wicking perpendicular to the warp wires and ethanol as the test liquid. Two additional tests were conducted in which the screen was inclined at 15^o to the gravity vector. The screens employed in these tests were 80×700 twilled-weave dutch with wicking parallel to the warp wires and 30×500 twilled-weave dutch with wicking perpendicular to the warp wires. In all cases, the line generated by the equation fit the data except at small values of $1/L$.

Effect of Evaporation on Experiment Data

If the assumption is made that wicking is occurring in the presence of uniform evaporation of the wicking liquid from the screen surface, the gravitational term of equation (5) will be unaffected by the phase change. Although the magnitude of the capillary

term may be altered since it has been shown that the dynamic contact angle may increase in this situation (ref. 4), the contact angle shall be assumed constant. The viscous term will obviously be affected since the velocity of the wicking liquid changes as the liquid leaves the screen by evaporation.

If a simple mass balance is used, the local velocity of the wicking liquid at any location between the liquid source and the leading edge of the wick may be given (see sketch (c)) as

$$V_x = \frac{dL}{dt} + \frac{\dot{G}(L - x)}{\rho A_F}$$

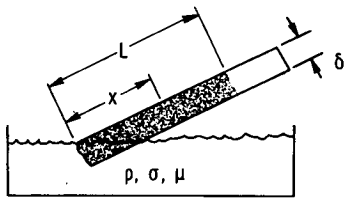

(c)

(i.e., the wicking velocity at any intermediate location x is greater than the velocity at the leading edge of the wick because the liquid evaporated between the two locations).

If the preceding equation is combined with the differential form of equation (3), we have

$$\frac{dP_f}{dx} = \frac{V_x A_F \mu}{K_1 A_T} = \frac{A_F}{A_T}\frac{\mu}{K_1}\left[\frac{dL}{dt} + \frac{\dot{G}(L - x)}{\rho A_F}\right]$$

Integrating the preceding expression for values of x from 0 to L yields

$$\Delta P_f = \frac{A_F}{A_T}\frac{\mu}{K_1}\left(L\frac{dL}{dt} + \frac{\dot{G}L^2}{2\rho A_F}\right)$$

The associated pressure balance may then be written as

$$\Delta P_c = \Delta P_f + \Delta P_g$$

$$\frac{\varphi\sigma}{D_s} = \frac{A_F \mu}{A_T K_1}\left(L\frac{dL}{dt} + \frac{\dot{G}L^2}{2\rho A_F}\right) + \rho a L \sin\alpha$$

Solving for L(dL/dt) yields

$$L\frac{dL}{dt} = \frac{\varphi\sigma}{D_s}\left(\frac{A_T}{A_F}\right)\frac{K_1}{\mu} - \frac{\rho a L K_1}{\mu}\left(\frac{A_T}{A_F}\right)\sin\alpha - \frac{\dot{G}L^2}{2\rho A_F}$$

or, in terms of c and V_w,

$$LV_w = c\left(\frac{\sigma}{\mu}\right) - c\left(\frac{\rho a}{\mu}\right)\left(\frac{D_s}{\varphi}\right)L\sin\alpha - \frac{\dot{G}L^2}{2\rho A_F} \tag{9}$$

This equation reduces to equation (5) when no evaporation occurs. However, in the presence of evaporation the wicking velocity observed at the wicking front would be decreased by evaporation, with the decrease being most pronounced at large values of L.

In order to ascertain if evaporation was a significant factor in the correlation constant obtained in this study, plots of LV_w against L^2 were made for each data run. If LV_w were constant (or nearly so) over the range of lengths examined in the horizontal or zero-gravity wicking tests, evaporative effects would be negligible. An examination of the data showed this to be true; thus, the obtained correlation constants are reliable.

Significance of Results

As discussed in the INTRODUCTION, wicking might be used to prevent localized drying out at the screen surface and the corresponding degradation of the retention characteristics of the screen. If it is assumed that all the incoming heat is used in vaporizing the liquid, we may write

$$\dot{Q} = \dot{m}\lambda$$

where $\dot{Q}$ is the applied heat rate, $\dot{m}$ is the mass rate leaving the surface by evaporation, and λ is the heat of vaporization.

Concentrated heat source. - If a concentrated heat source is acting along a line at some distance L from the liquid source or pool, it is possible to use the preceding to write an equation which expresses the maximum local heat rate which can be accommodated as a function of distance from the liquid source in zero gravity.

$$\dot{Q} = \rho A_F V_w \lambda = \rho A_F \lambda \frac{c}{L}\left(\frac{\sigma}{\mu}\right) \tag{10}$$

This assumes the entire mass of liquid which can be supplied at L is being evaporated instantaneously. The flow area A_F is impossible to calculate rigorously because of the complex nature of the wicking process. However, an estimate of the magnitude of the term can be made by expressing A_F as some fraction of the total cross-sectional area of the screen (i.e., $A_F = 0.5\ W\delta$). Thus, equation (10) can be written as

$$\frac{\dot{Q}}{W} = 0.5\ \delta\rho\lambda\ \frac{c}{L}\left(\frac{\sigma}{\mu}\right)$$

With liquid hydrogen as the liquid, the solutions are plotted in figure 11 for 200×1400, 80×700, and 30×500 twilled-weave dutch screens with wicking flow running perpendicular to the warp wires. Calculated heat rates of 1.4×10^{-3} to 2.9×10^{-2} J/sec/cm (0.0146 to 3.02 Btu/hr/ft) can be accommodated by wicking flow if the heat source is within 28 centimeters (approx. 11 in.) from the liquid source. If liquid oxygen were the liquid, the acceptable heat rate would be about three times as large since $(\sigma/\mu)\rho\lambda$ for liquid oxygen is roughly three times that for liquid hydrogen.

Uniform heat source. - If it is assumed that the screen surface is experiencing a uniform heat loading along its length, equation (9), presented in the section Effect of Evaporation on Experiment Data, may be used to determine the point or location at which screen dryout will occur. Assume that wicking is occurring in a weightless environment (or in a horizontally oriented screen). By allowing $V_w = 0$, the length of screen which remains sealed over because of wicking may be determined as a function of the evaporation rate per unit length of screen. Equation (9) may be written

$$\frac{c}{L}\left(\frac{\sigma}{\mu}\right) = \frac{\dot{G}L}{2\rho A_F}$$

or

$$\dot{G} = 2\rho A_F\left(\frac{c}{L^2}\right)\left(\frac{\sigma}{\mu}\right) \tag{11}$$

Equation (11) expresses the relation between evaporation rate per unit length and wetted length of screen. If it is again assumed that all incoming heat is used in the evaporation of the liquid, equation (11) may be rewritten as

$$\dot{G} = \frac{\dot{Q}}{\lambda L}$$

$$\dot{Q} = 2\rho\lambda A_F \left(\frac{c}{L}\right)\frac{\sigma}{\mu}$$

Expressing A_F as before and dividing both sides of the expression by A_S [$A_S = W(2L)$] yield

$$\frac{\dot{Q}}{A_S} = \frac{\rho\lambda\delta}{2}\left(\frac{c}{L^2}\right)\left(\frac{\sigma}{\mu}\right)$$

This relation can then be employed to estimate the wetted length of the screen as a function of the applied heat rate per unit area of screen surface. Solutions to the equation using liquid hydrogen are plotted in figure 12 for 200×1400, 80×700, and 30×500 twilled-weave dutch screen with the wicking flow running perpendicular to the warp wires. For an applied heat rate of 3.93×10^{-4} to 8.1×10^{-3} J/sec/cm^2 (0.0409 to 0.845 Btu/hr/ft^2), the screen will become dry at a distance of 10 centimeters (4 in.) from the liquid source. Again if liquid oxygen were the liquid, heat rates would be about three times as great for a given length of wetted screen.

CONCLUDING REMARKS

This investigation was performed to determine the magnitude of the wicking rates of liquids in screens. The study consisted of the development of an analytical model, as well as the experimental investigation required to support the analysis.

The majority of the tests were conducted either in weightlessness (providing the total wicked distance was sufficient to obtain measurements) or in a chamber in which the screens were oriented horizontally to simulate zero-gravity wicking. In addition, several tests were conducted in which the screen was inclined at some angle to the gravity vector. A series of eight twilled-weave dutch, two plain-weave dutch, and three square-mesh screens were tested. The twilled-weave and plain-weave dutch screens were tested both with the warp wire running parallel to the flow direction of the wicking liquid and with the warp wire running perpendicular to the flow direction of the wicking liquid. Two liquids (methanol and ethanol) were used as the wicking liquids. These liquids had a near zero-degree static contact angle on the screen material to duplicate the contact angle of typical propellants on screen material.

The results of the experiments showed that the analytical model developed was successful in predicting the correct functional dependence of several parameters important in the wicking process, in particular, distance from the liquid source, liquid properties, and gravitational effects. Because the geometry of the pores in the screen was complex,

it was necessary to lump several screen geometric parameters into a single geometric constant in the derived expression for the wicking velocity. This constant was empirically determined for each twilled-weave and plain-weave dutch screen. Additionally, the magnitude of this constant was shown to be unaffected by evaporation over the range of parameters investigated in this study during horizontal wicking in normal gravity. When the constants are known, the derived equation can be used to predict the magnitude of the wicking velocity for any liquid in the screens tested. Additionally, experiments showed that square-mesh screens do not wick and that, as expected, wicking rates in horizontally oriented screens in normal gravity are identical to those obtained in zero gravity.

Although the observed wicking rates were small, a worst-case analysis made by a simple mass balance shows that they may be used to maintain the screen pores in a filled condition in response to small heat fluxes, provided the incoming heat is within a short distance from the liquid source. Furthermore, since the observed wicking rates were generally small, they should not cause excess quantities of vapor to be trapped in the acquisition device during filling.

Lewis Research Center,
National Aeronautics and Space Administration,
Cleveland, Ohio, January 4, 1974,
502-24.

APPENDIX - TEST FACILITY

The zero-gravity data for this study were obtained in the Lewis 2.2-Second Drop Tower Facility. A schematic diagram of the facility is shown in figure 13. The facility consists of a building 6.4 meters (21 ft) square by 30.5 meters (100 ft) tall. Contained within this building is a drop area 27 meters (89 ft) long with a cross section of 1.5 meters by 2.75 meters (5 ft by 9 ft).

The service building has, as its major elements, a shop and service area, a calibration room, and a controlled-environment room. Those components of the experiment that require special handling are prepared in the controlled-environment room of the facility. This air-conditioned and filtered room contains an ultrasonic cleaning system and the laboratory equipment necessary for the handling of test liquids (fig. 14).

Mode of Operation

A 2.2-second period of weightlessness is obtained by allowing the experiment package to fall from the top of the drop area. In order to minimize air drag on the experiment package, it is enclosed in a drag shield that is designed with a high ratio of weight to frontal area and a low drag coefficient. The relative motion of the experiment package with respect to the drag shield during a test is shown in figure 15. Throughout the test, the experiment package and drag shield fall freely and independently of each other; that is, no guide wires, electrical lines, and so forth, are connected to either. Therefore, the only force acting on the freely falling experiment package is the air drag associated with the relative motion of the package within the enclosure of the drag shield. This air drag results in an equivalent gravitational acceleration acting on the experiment which is estimated to be below 10^{-5} g's.

Release System

The experiment package, installed within the drag shield, is suspended at the top of the drop area by a highly stressed music wire which is attached to the release system. This release system consists of a double-acting air cylinder with a hard steel knife edge which is attached to the piston. Pressurization of the air cylinder drives the knife edge against the wire, which is backed by an anvil. The resulting notch causes the wire to fail and smoothly release the experiment. No measurable disturbances are imparted to the package by this release procedure.

Recovery System

After the experiment package and drag shield have traversed the total length of the drop area and have been decelerated in a 2.2-meter (7-ft) deep container filled with sand, they are recovered. The deceleration rate (average 15 g's) is controlled by selectively varying the tips of the deceleration spikes mounted on the bottom of the drag shield (fig. 15). At the time of impact of the drag shield in the decelerator container, the experiment package has traversed the vertical distance within the drag shield (compare figs. 15(a) and (c)).

REFERENCES

1. Blatt, M. H.; Stark, J. A.; and Siden, L. E.: Low Gravity Propellant Control Using Capillary Devices in Large Scale Cryogenic Vehicles. Rep. GDC-DDB 70-007, General Dynamics/Convair (NASA CR-102900), Aug. 1970.

2. Anon.: Low-G Fluid Behavior and Control. Rep. R-71-48631-003, Martin-Marietta Co., 1971.

3. Graumann, D. W.; Soliman, M. M.; and Berenson, P. J.: Wicking Evaporative Heat Exchangers. Rep. 70-6190, AiResearch Mfg. Co. (NASA CR-108488), May 28, 1970.

4. Frohnsdorff, Geoffrey; and Tejada, Silvestre: Measurement of Contact Angles and Evaluation of Surface Coatings. Gillette Research Inst., Inc. (NASA CR-72975), Aug. 1971.

5. Cady, E. C.: Study of Thermodynamic Vent and Screen Baffle Integration for Orbital Storage and Transfer of Liquid Hydrogen. McDonnell Douglas Astronautics Co. (NASA CR-134482), Aug. 1973.

TABLE I. - LIQUID PROPERTIES AT 20° C

Liquid	Surface tension, σ, N/cm	Density, ρ, g/cm^3	Absolute viscosity, μ, g/cm/sec
Ethanol	22.3×10^{-5}	0.789	1.200×10^{-2}
Methanol	22.6	.793	.597

TABLE II. - WICKING FLOW AND SCREEN GEOMETRY

Screen mesh	Manufacturer's rated pore size[a], D_s, μm	Screen thickness, δ, μm	Calculated porosity, p	Direction of wicking in relation to warp wire	Correlation constant, c, μm
20×250 Twilled-weave dutch	80	685	0.399	Perpendicular Parallel	1.7 3.4
24×110 Plain-weave dutch	138	940	[b]0.622	Perpendicular Parallel	2.5 1.5
50×250 Plain-weave dutch	65	368	[b]0.665	Perpendicular Parallel	1.6 .67
30×500 Twilled-weave dutch	57	430	0.428	Perpendicular Parallel	0.71 3.7
165×800 Twilled-weave dutch	37	147	0.533	Perpendicular Parallel	1.6 .48
200×600 Twilled-weave dutch	30	135	0.614	Perpendicular Parallel	0.97 .50
80×700 Twilled-weave dutch	40	254	0.368	Perpendicular Parallel	0.42 .87
165×1400 Twilled-weave dutch	21	147	0.348	Perpendicular Parallel	0.19 .38
200×1400 Twilled-weave dutch	14	135	0.272	Perpendicular Parallel	0.11 .34
325×2300 Twilled-weave dutch	10	61	0.252	Perpendicular Parallel	0.11 .17

[a]From ref. 5.
[b]Measured.

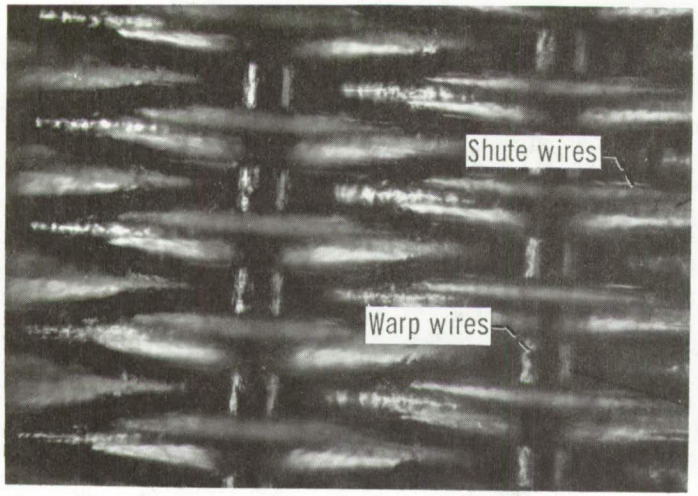

(a) 50x250 Plain-weave dutch.

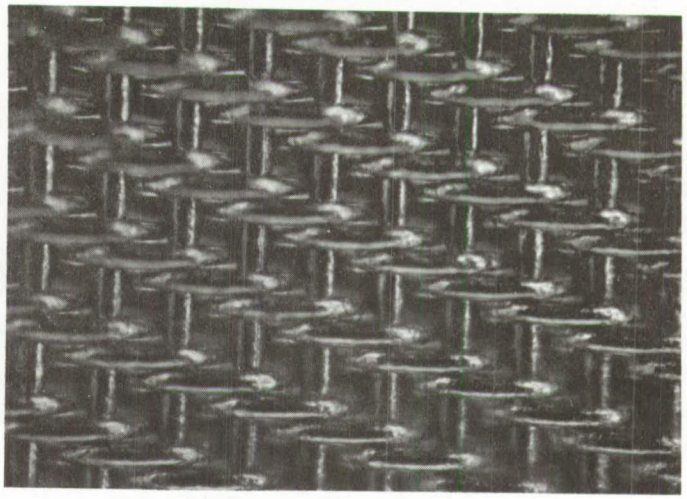

(b) 200x600 Twilled-weave dutch.

(c) 80x700 Twilled-weave dutch.

Figure 1. - Screen samples. X100.

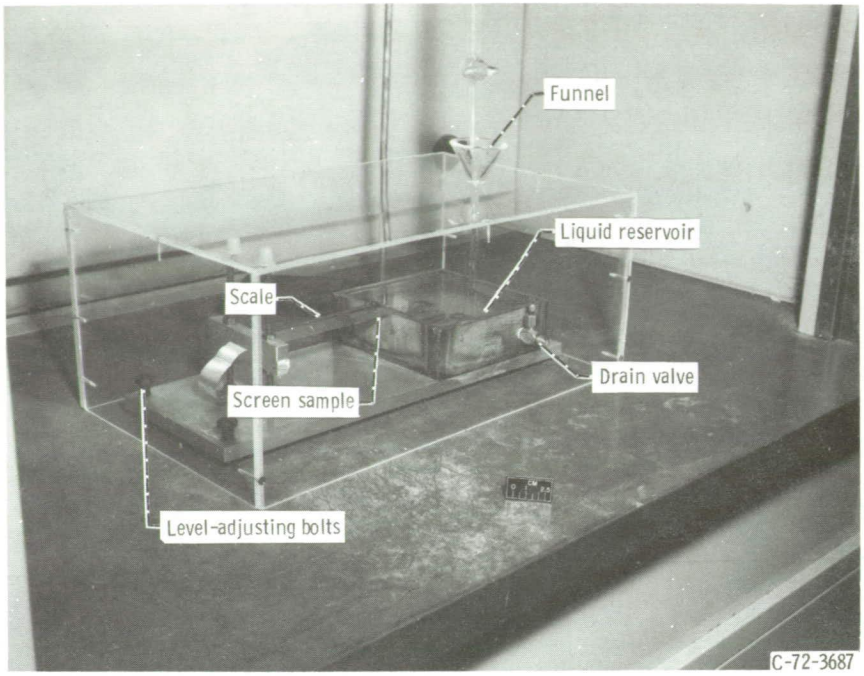

Figure 2. - Horizontal wicking chamber.

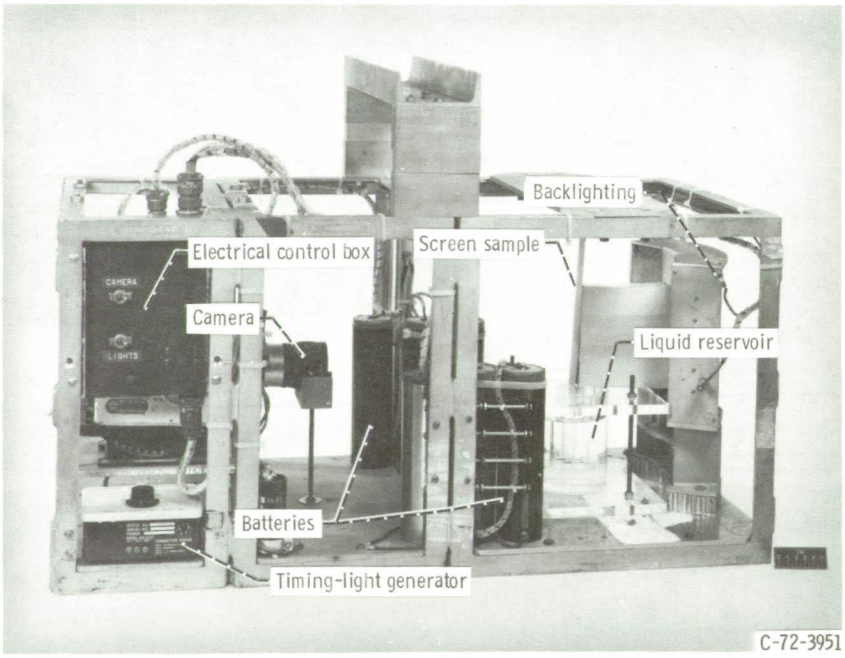

Figure 3. - Experiment drop package.

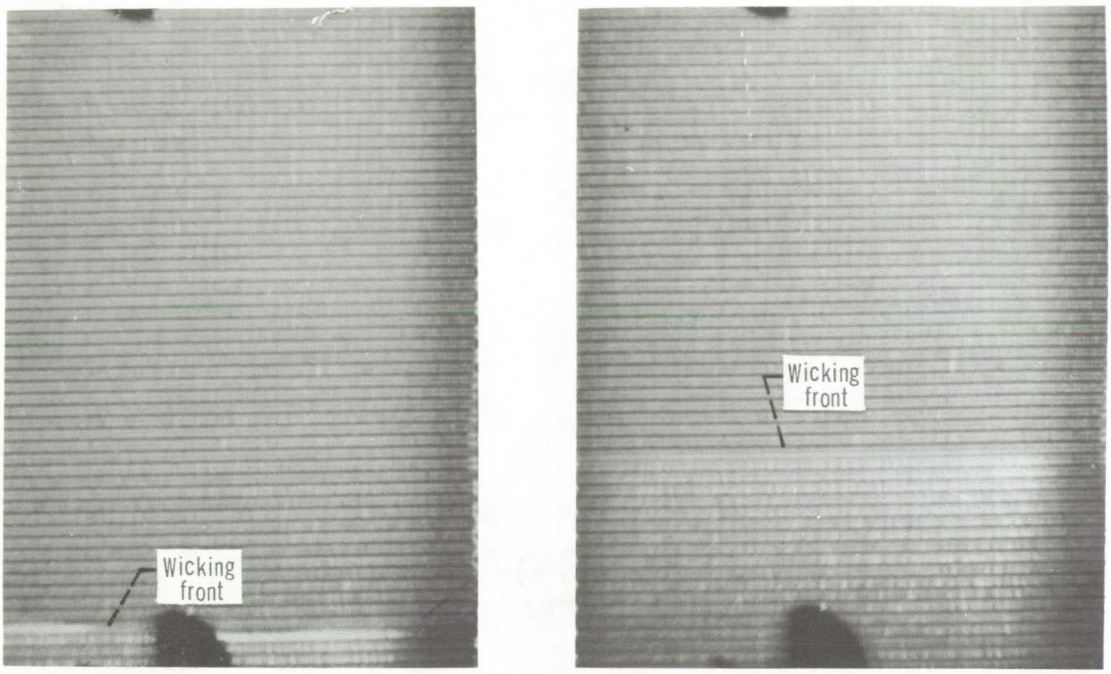

(a) 50x250 Plain-weave dutch screen; wicking perpendicular to warp wires; wicking height differential, ΔL, 0.76 cm; time differential, Δt, 1.13 seconds.

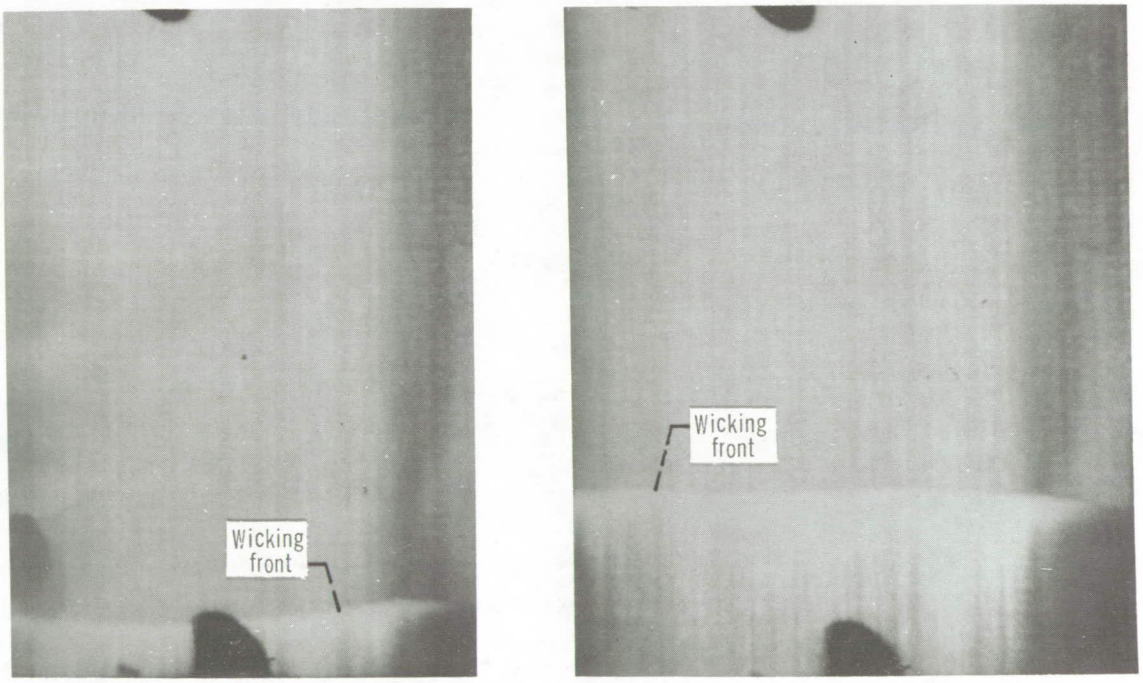

(b) 200x600 Twilled-weave dutch screen; wicking perpendicular to warp wires; wicking height differential, ΔL, 0.55 cm; time differential, Δt, 0.94 seconds.

Figure 4. - Wicking in weightlessness.

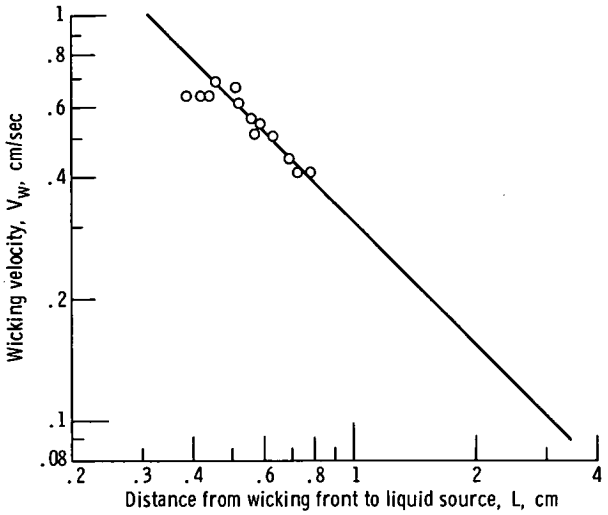

Figure 5. - Wicking velocity in weightlessness as function of distance from liquid source. 80x700 Twilled-weave dutch screen; wicking flow parallel to warp wires; test liquid, methanol.

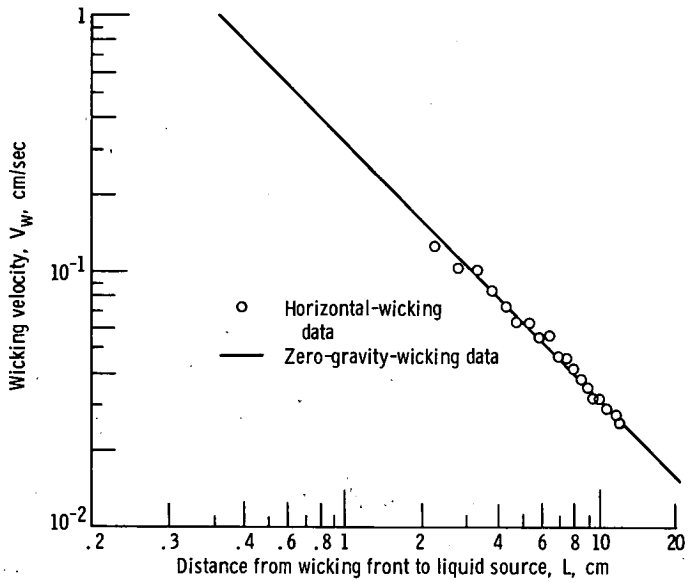

Figure 6. - Comparison of wicking velocities in horizontally oriented screen with those in weightlessness. 80x700 Twilled-weave dutch screen; wicking flow parallel to warp wires; test liquid, methanol.

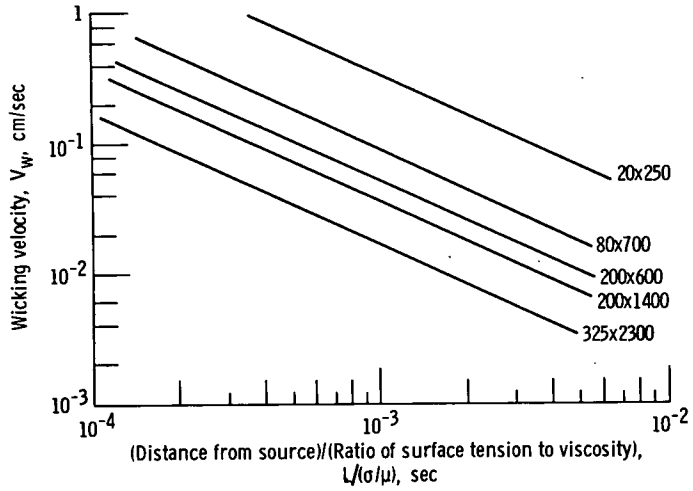

Figure 7. - Comparison of wicking rates for various twilled-weave dutch screens with wicking flow parallel to warp wires.

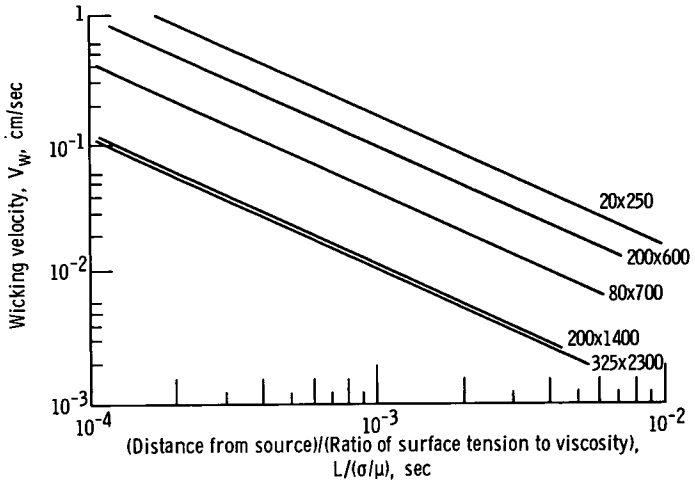

Figure 8. - Comparison of wicking rates for various twilled-weave dutch screens for wicking flow perpendicular to warp wires.

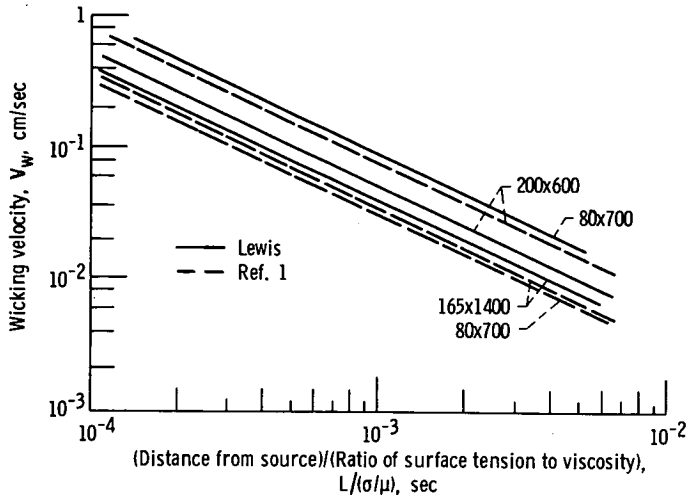

Figure 9. - Comparison of Lewis data with data of reference 1. Wicking flow parallel to warp wires.

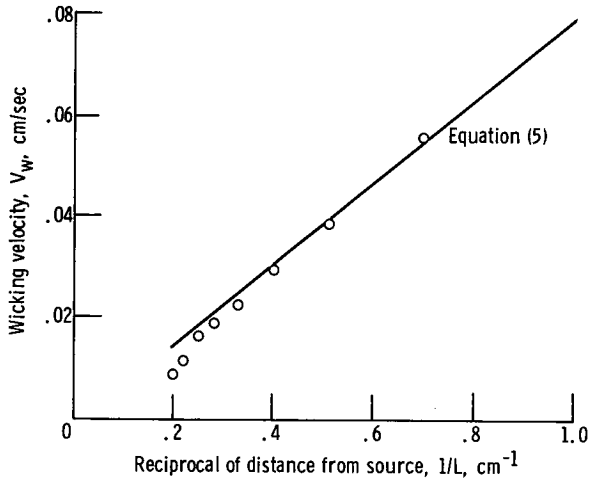

Figure 10. - Wicking velocity as a function of reciprocal of distance from the liquid source, for a vertically oriented screen. 80x700 Twilled-weave dutch screen; wicking flow perpendicular to warp wires; test liquid, ethanol.

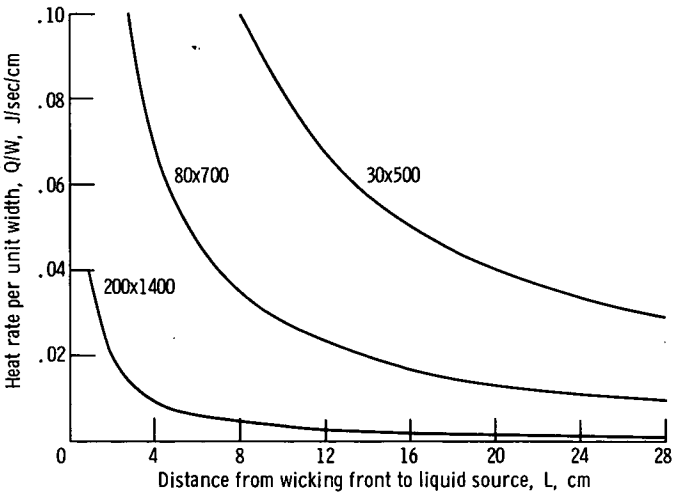

Figure 11. - Acceptable local incident heat flux as function of distance from liquid source. Wicking flow perpendicular to warp wires; test liquid, hydrogen.

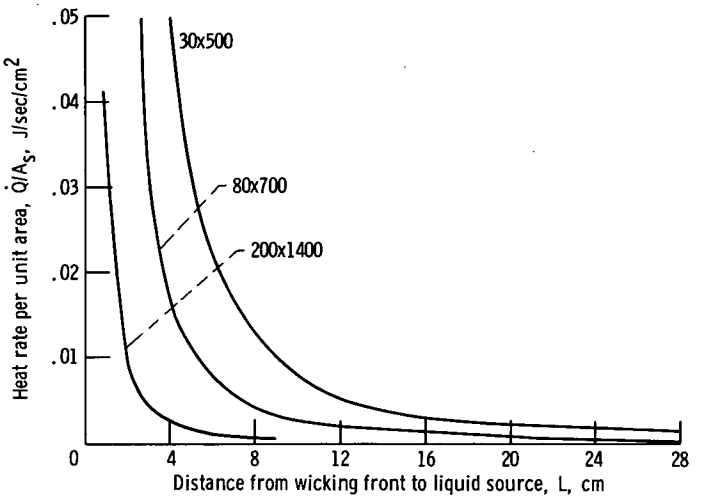

Figure 12. - Maximum uniform heat flux as function of distance from liquid source. Wicking flow perpendicular to warp wires; test liquid, hydrogen.

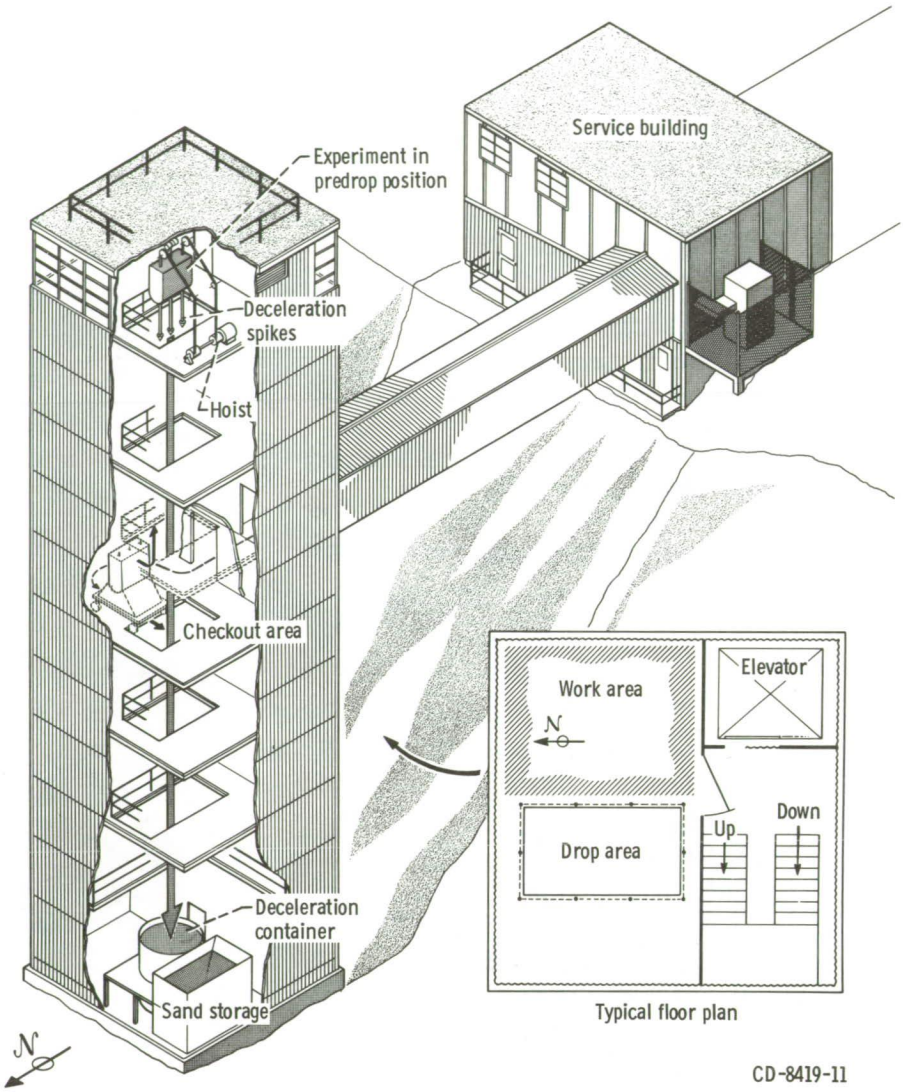

Figure 13. - 2.2-Second Drop Tower Facility.

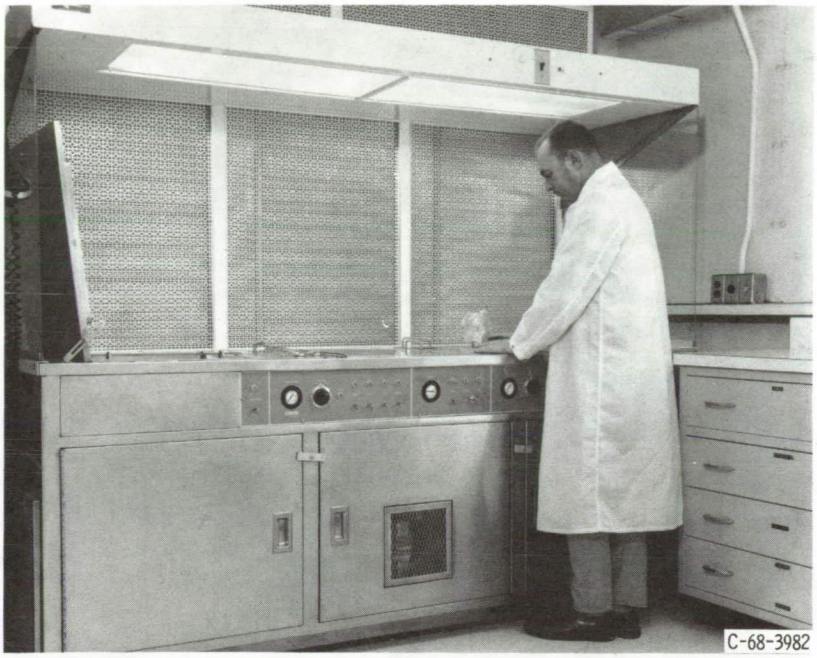

(a) Ultrasonic cleaning system.

(b) Laboratory equipment.

Figure 14. - Controlled-environment room.

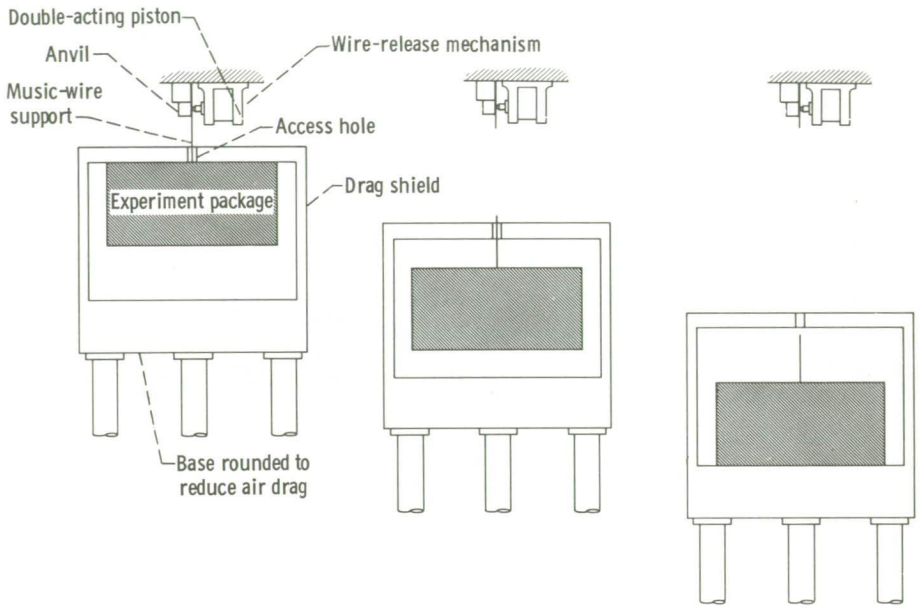

Figure 15. - Position of experiment package and drag shield before, during, and after test drop.